J. Fluid Mech. (2010), *vol.* 643, *pp.* 207–232.
doi:10.1017/S0022112009992096

Solving the nonlinear shallow-water equations in physical space

M. ANTUONO[1]† AND M. BROCCHINI[2]

[1]INSEAN (The Italian Ship Model Basin), via di Vallerano 139, 00128 Rome, Italy

[2]Dipartimento ISAC, Università Politecnica delle Marche, via Brecce Bianche 12, 60131 Ancona, Italy

(Received 16 March 2009; revised 7 September 2009; accepted 7 September 2009; first published online 23 December 2009)

The boundary value problem for the nonlinear shallow-water equations with a beach source term is solved by direct use of physical variables, so that solutions are more easily inspected than those obtained by means of hodograph transformations. Beyond an overall description of the near-shoreline flows in terms of the nonlinear shallow-water equations, significant results are provided by means of a perturbation approach which enables much of the information on the flow to be retained. For sample waves of interest (periodic and solitary), first-order solutions of the shoreline motion and of the near-shoreline flows are computed, illustrated and successfully compared with the equivalent ones obtained through a hodograph transformation method previously developed by the authors. Wave–wave interaction, both at the seaward boundary and within the domain, is also accurately described. Analytical conditions for wave breaking within the domain are provided. These, compared with the authors' hodograph model, show that the first-order condition of the present model is comparable to the second-order condition of that model.

Key words: solitary waves, surface gravity waves, wave breaking

1. Introduction and background

Near-shoreline flows induced by long waves propagating on a frictionless sloping beach of constant slope are traditionally studied by means of the nonlinear shallow-water equations (NSWEs; Carrier & Greenspan 1958; Shen & Meyer 1963; Tuck & Hwang 1972; Meyer 1986*a*; Brocchini & Peregrine 1996; Pritchard & Dickinson, 2007).

The aim of the present paper is the solution of the boundary value problem (BVP) for the NSWE with a beach source term by direct use of the physical variables, i.e. without resorting to hodograph transformations such as those performed by Antuono & Brocchini (2007). Hence, though the global framework for the solution of this very recently tackled problem is the same, the present solution has the major advantage of being formulated in variables which are more easily inspected.

This is achieved first by providing a clear overall description of the flow in terms of the NSWEs and subsequently by using a perturbation approach in the (x, t)-space, which properly accounts for nonlinear contributions at the desired order of accuracy.

† Email address for correspondence: matteoantuono@gmail.com

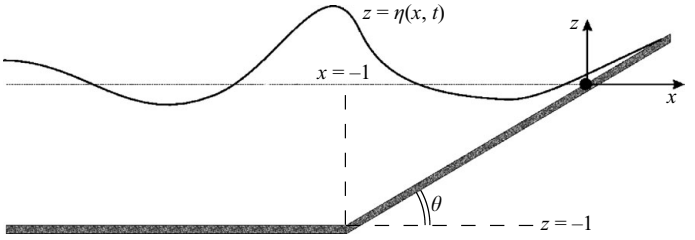

FIGURE 1. Sketch of the geometry and the flow dimensionless variables for the beach problem.

1.1. *The nonlinear shallow-water equations*

The NSWEs, in dimensionless form, read

$$\left.\begin{aligned} &d_t + (u\,d)_x = 0, \\ &u_t + u\,u_x + d_x + 1 = 0, \end{aligned}\right\} \tag{1.1}$$

in which u is the onshore velocity; $d=\eta - x$ is the depth; η is the free-surface elevation; and the notation $(\,)_i$ indicates partial differentiation with respect to the variable 'i'. The axes origin is posed at the undisturbed shoreline; the x-coordinate gives the onshore direction and points in the landward direction, with (x, z) forming a right-handed reference frame (figure 1). The above equations have been cast in dimensionless form using the scale factors of Brocchini & Peregrine (1996):

$$d = d^*/d_0^*, \quad u = u^*/\sqrt{g\,d_0^*}, \quad x = x^*\,\tan(\theta)/d_0^*, \quad t = t^*\tan(\theta)\sqrt{g/d_0^*}, \tag{1.2}$$

in which the variables with the superscript '*' represent the dimensional quantities; d_0^* is the still-water depth at the seaward boundary of the sloping region; g is the gravity acceleration; $\tan(\theta)$ is the beach slope; and θ is the beach angle with respect to the x-axis.

System (1.1) is hyperbolic, and its characteristic form is

$$\left.\begin{aligned} \mathrm{d}\alpha/\,\mathrm{d}t = 0 \qquad &\text{on curves such that} \quad \mathrm{d}x/\,\mathrm{d}t = u + c, \\ \mathrm{d}\beta/\,\mathrm{d}t = 0 \qquad &\text{on curves such that} \quad \mathrm{d}x/\,\mathrm{d}t = u - c, \end{aligned}\right\} \tag{1.3}$$

$$\text{in which} \quad c = \sqrt{d} \quad \text{and} \quad \alpha = 2c + u + t, \quad \beta = 2c - u - t. \tag{1.4}$$

The variables α and β are the so-called Riemann invariants, since they do not change their value along the special curves in (1.3) known as 'characteristics'. Assuming the flow to be subcritical (that is $u + c > 0$ and $u - c < 0$), the first type of characteristic curves propagates signals towards the shore, while the second type propagates signals offshore. We name the first and the second characteristics of (1.3) 'incoming' and 'outgoing' respectively. By defining the shoreline as the curve along which $d = 0$, that is $c = 0$, all characteristic curves coincide with this special curve except when bores meet the shoreline, a case which is not considered here. Let $x = x_s(t)$ denote the shoreline position ('s' is for 'at the shoreline'). Since the shoreline separates the wet part of the domain from the dry one, it also follows that

$$\mathrm{d}x_s/\mathrm{d}t = u_s(t), \quad \text{where} \quad u_s(t) \equiv u(x_s(t), t). \tag{1.5}$$

The shoreline's velocity equals the velocity of the fluid particle at the shoreline; so these velocities have the same horizontal component, as stated in (1.5).

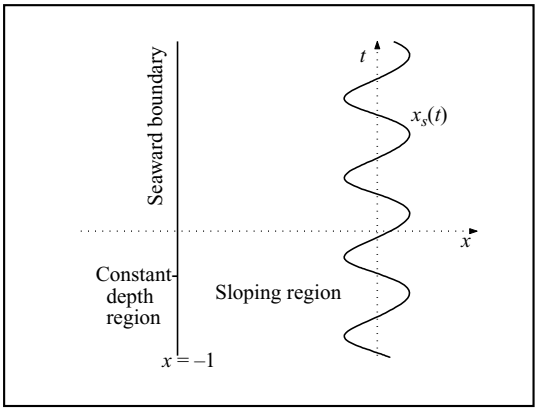

FIGURE 2. Sketch of the domain in the (x, t)-plane for the BVP.

1.2. *The boundary value problem*

We want to solve the BVP for the NSWEs; that is to say we want to find a solution of (1.1) in the domain $(x, t) \in (-1, x_s(t)) \times \mathbb{R}$ assigning data (η, u) at the seaward boundary of the sloping beach, i.e. at $x = -1, \forall t \in \mathbb{R}$ (see figures 1 and 2). We limit our attention to non-breaking waves, although we try to extend some results also to breaking waves. In §§ 2 and 3 we use a perturbation expansion starting from the assumption of small data at the seaward boundary. This hypothesis includes the case of non-breaking waves and, moreover, is not restrictive, since waves entering the sloping region amplify in such a region because of shoaling effects. The perturbation parameter is $\epsilon = H^*/d_0^*$ in which H^* is the wave height and d_0^* is the still-water depth, both evaluated at the seaward boundary. Hence, we say a wave is 'small' if $\epsilon \ll 1$ (i.e. if its height is small in comparison with the local depth, which implies that $\eta = O(\epsilon) \ll 1$ at the seaward boundary). Moreover, balancing the continuity equation (first in (1.1)), we also get $u = O(\epsilon)$ at the seaward boundary. Note that the hypothesis $\epsilon \ll 1$ is a good assumption only if H^* and d_0^* are evaluated at the seaward boundary. Indeed, near the shoreline (where $d \ll 1$), d_0^* can have the same order as H^*, and then we would obtain $\epsilon = O(1)$. (This observation is based on the analyses proposed in Bellotti & Brocchini 2002.) This also implies that we cannot linearize the NSWEs, since the linearization would be well posed only if $\epsilon \ll 1$ in the entire sloping region. Such a result also means that the propagation of waves near the shore is an intrinsically nonlinear phenomenon.

For these reasons, in the following we use the NSWEs without applying any linearization and define proper perturbation expansions, applied to the characteristic paths (§ 2) based only on data at the seaward boundary (i.e. based only on the parameter $\epsilon \ll 1$). This ensures that the solution, given in terms of the dependent variables u and η and illustrated in § 3, preserves its nonlinear nature and gives uniform ϵ-expansions, i.e. expansions valid all over the domain.

2. The governing equation

If we express the dependent variables u, η through the Riemann invariants α, β, we can rewrite the first two equations of (1.3) as follows:

$$\left.\begin{array}{ll} \alpha = \text{constant} & \text{on curves such that } \dfrac{\mathrm{d}x}{\mathrm{d}t} = \dfrac{3\alpha - \beta}{4} - t, \\ \beta = \text{constant} & \text{on curves such that } \dfrac{\mathrm{d}x}{\mathrm{d}t} = \dfrac{\alpha - 3\beta}{4} - t. \end{array}\right\} \tag{2.1}$$

In the (x,t)-plane each characteristic curve is parameterized by t and labelled by the initial time t_0 defined to be where the characteristic meets $x=-1$. Hence, we pose $x=\phi(t,t_0)$, and for the sake of brevity, we introduce the notation $t_0\equiv y$. We have $\alpha=\alpha_0(y)\equiv 2c(-1,y)+u(-1,y)+y$ along the incoming characteristic curves and $\beta=\beta_0(y)\equiv 2c(-1,y)-u(-1,y)-y$ along the outgoing characteristic curves; α_0 and β_0 are our data. Then we can write

$$\left.\begin{aligned} &\alpha=\alpha_0 \quad \text{on curves such that} \quad \phi_t=\frac{3\alpha_0-\beta}{4}-t,\\ &\beta=\beta_0 \quad \text{on curves such that} \quad \phi_t=\frac{\alpha-3\beta_0}{4}-t. \end{aligned}\right\} \tag{2.2}$$

Since the boundary values are carried by the incoming characteristic curves, we limit our attention to them and obtain a closed equation for their motion. In the following we show that our choice is sufficient to describe the global flow evolution.

We start by rewriting the first expression of (2.2) as follows:

$$\phi_t=\frac{3\,\alpha_0-\beta}{4}-t \quad \Rightarrow \quad \beta=3\,\alpha_0-4(\phi_t+t). \tag{2.3}$$

In this case it is $\beta=\beta(\phi,t)$, since we are 'moving' along an incoming characteristic curve. Then, taking the total t-derivative of β, we have

$$\dot\beta=\beta_t+\phi_t\beta_x=\beta_t+\left(\frac{3\alpha_0-\beta}{4}-t\right)\beta_x, \tag{2.4}$$

while using (2.3) we obtain

$$\dot\beta=-4(\phi_{tt}+1). \tag{2.5}$$

The y-derivative of (2.3) gives

$$\frac{\partial}{\partial y}(\beta)=\beta_x\phi_y=3\dot\alpha_0-4\phi_{ty} \quad \Rightarrow \quad \beta_x=\frac{3\dot\alpha_0-4\phi_{ty}}{\phi_y}, \tag{2.6}$$

where all the derivatives of β are evaluated at $x=\phi(t,y)$. Now we only need an explicit expression for β_t. We can obtain it by rewriting the second expression of (1.3) in the following way:

$$\beta_t+(u-c)\beta_x=\beta_t+\left(\frac{\alpha-3\beta}{4}-t\right)\beta_x=0. \tag{2.7}$$

Since this equation is valid for all $(x,t)\in(-1,x_s(t))\times\mathbb{R}$, it is also valid along $x=\phi$. Then, we can evaluate (2.7) at $x=\phi$, obtaining

$$\beta_t+\left(\frac{\alpha_0-3\beta}{4}-t\right)\beta_x=0 \tag{2.8}$$

from which we get the required expression of β_t. Combining (2.3)–(2.6) into (2.8), we obtain the following differential equation for the incoming characteristic curves:

$$2\phi_y(\phi_{tt}+1)=(4\phi_{ty}-3\dot\alpha_0)(\alpha_0-t-\phi_t). \tag{2.9}$$

The BVP we are solving is then

$$\left.\begin{aligned} &2\phi_y(\phi_{tt}+1)=(4\phi_{ty}-3\dot\alpha_0)(\alpha_0-t-\phi_t) \quad \text{for } t>y,\\ &\phi|_{t=y}=-1,\\ &\phi_t|_{t=y}=\frac{3\alpha_0-\beta_0}{4}-y. \end{aligned}\right\} \tag{2.10}$$

It is simple to prove that the equation for the outgoing curve can be obtained from (2.9) by replacing α_0 with $-\beta_0$. The meaning of this is explained in the following section.

2.1. *A trivial solution of (2.10)*

We can test (2.10) using the simplest known analytical solution for the NSWEs, i.e. the solution in the trivial case of no motion ($u = \eta \equiv 0$) for which we get (see (1.4))

$$\alpha = 2\sqrt{-x} + t, \quad \beta = 2\sqrt{-x} - t \tag{2.11}$$

and the following boundary data ($x = -1$ and $t = y$):

$$\alpha_0 = 2 + y, \quad \beta_0 = 2 - y. \tag{2.12}$$

For the incoming/outgoing characteristic curves we obtain, respectively,

$$x = -\frac{(t-\alpha_0)^2}{4}, \quad x = -\frac{(t+\beta_0)^2}{4}. \tag{2.13}$$

Then, the incoming curves can be expressed in the following way:

$$\phi(t, y) = -\frac{(t-y-2)^2}{4}. \tag{2.14}$$

It is simple to verify that (2.14) is a solution of (2.10). Further, the curves appearing in (2.13) coincide for $\beta_0 = -\alpha_0$, which happens when the incoming curves reach the still-water shoreline at $x = 0$. This result is not restricted to the trivial case, since it is always true that $\beta = -\alpha$ at the shoreline. Along this special curve all the characteristic curves (incoming, outgoing) coincide, and thus, the shoreline can be seen as the envelope of the characteristic curves themselves. Moreover, it implies that the incoming curve (carrying α_0) and the outgoing curve (carrying $\beta_0 = -\alpha_0$) can be seen as branches of a unique curve which goes from the seaward boundary up to the shoreline where is reflected. This supports our choice of studying only the incoming curves and suggests the use of only one datum, i.e. α_0, regarding β_0 as an unknown function of this datum. From a physical point of view, this means that α is carrying information coming from the ocean into the sloping region, while β is carrying information on the presence of the shoreline out of the sloping region.

2.2. *A perturbation expansion*

Apart from the trivial case above, the direct solution of the boundary problem (2.10) might be prohibitive because of the high nonlinearity of the equation for ϕ. Thus, we choose to apply a perturbation method on the boundary data, which enables us to find a simplified solution. Hence, we assume our data to be 'small', and we expand it in series of a small parameter ϵ:

$$\alpha_0 = \alpha_{0,0} + \epsilon\alpha_{0,1} + \epsilon^2\alpha_{0,2} + O(\epsilon^3) \tag{2.15}$$

in which $\alpha_{0,0} = 2 + y$. Similarly we can suppose the solution of (2.10) to be 'near' the trivial one; then we assume the following expansion for ϕ:

$$\phi = \phi^{(0)} + \epsilon\phi^{(1)} + \epsilon^2\phi^{(2)} + O(\epsilon^3) \tag{2.16}$$

in which $\phi^{(0)}$ is given by (2.14). Substituting (2.15) and (2.16) into (2.9), we obtain at the first order in ϵ:

$$(t-y-2)\left(\phi^{(1)}_{tt} + 2\phi^{(1)}_{ty}\right) - \phi^{(1)}_t + \phi^{(1)}_y + \alpha_{0,1} - \frac{3}{2}(t-y-2)\dot{\alpha}_{0,1} = 0. \tag{2.17}$$

The factor $(t-y-2)$ is a 'trace' of the undisturbed shoreline $x_s=0$, since in the trivial case the characteristic curves reach it when $(t-y-2)=0$. Putting $\psi^{(1)}=\phi^{(1)}-(t-y-2)\alpha_{0,1}/2$, we get

$$(t-y-2)\left(\psi^{(1)}_{tt}+2\psi^{(1)}_{ty}\right)-\psi^{(1)}_{t}+\psi^{(1)}_{y}=0. \tag{2.18}$$

Then, we make the following change of variables:

$$\left.\begin{array}{ll} \tau=t-y-2, & \dfrac{\partial}{\partial t}=\dfrac{\partial}{\partial \tau}, \\ \xi=y \quad \Rightarrow & \dfrac{\partial}{\partial y}=-\dfrac{\partial}{\partial \tau}+\dfrac{\partial}{\partial \xi}. \end{array}\right\} \tag{2.19}$$

Now, the domain is $(\tau,\xi)\in(-2,+\infty)\times\mathbb{R}$ and (2.18) becomes

$$\tau\left(2\psi^{(1)}_{\tau\xi}-\psi^{(1)}_{\tau\tau}\right)-2\psi^{(1)}_{\tau}+\psi^{(1)}_{\xi}=0. \tag{2.20}$$

Applying the Fourier transform $\mathscr{F}$ with respect to the ξ variable, we obtain

$$\tau\left(2is\chi^{(1)}_{\tau}-\chi^{(1)}_{\tau\tau}\right)-2\chi^{(1)}_{\tau}+\mathrm{i}s\chi^{(1)}=0, \tag{2.21}$$

in which $\chi^{(1)}(\tau,s)=\mathscr{F}(\psi^{(1)}(\tau,\cdot))(s)$. The only regular (i.e. bounded, continuous and differentiable) solution for (2.21) is

$$\chi^{(1)}(\tau,s)=\exp(\mathrm{i}s\tau)A_1(s)[J_0(s\tau)-\mathrm{i}J_1(s\tau)], \tag{2.22}$$

and therefore, we obtain

$$\phi^{(1)}(\tau,\xi)=\frac{1}{2\pi}\int_{\mathbb{R}}\mathrm{e}^{\mathrm{i}s(\tau+\xi)}A_1(s)[J_0(s\tau)-\mathrm{i}J_1(s\tau)]\,\mathrm{d}s+\frac{\tau}{2}\alpha_{0,1}, \tag{2.23}$$

in which $J_n(x)$ is the Bessel function of the first kind and of the nth order, and the integration is carried out for s varying from $-\infty$ to $+\infty$.

At the second order in ϵ it is

$$(t-y-2)\left(\phi^{(2)}_{tt}+2\phi^{(2)}_{ty}\right)-\phi^{(2)}_{t}+\phi^{(2)}_{y}+\alpha_{0,2}-\frac{3}{2}(t-y-2)\dot{\alpha}_{0,2}+F=0, \tag{2.24}$$

in which F is a source term which has the form

$$F(t,y)=2\phi^{(1)}_{y}\phi^{(1)}_{tt}+\left(3\dot{\alpha}_{0,1}-4\phi^{(1)}_{yt}\right)\left(\alpha_{0,1}-\phi^{(1)}_{t}\right). \tag{2.25}$$

Following the previously described procedure, we obtain

$$\begin{aligned}\phi^{(2)}(\tau,\xi)=&\frac{1}{2\pi}\int_{\mathbb{R}}\exp[\mathrm{i}s(\tau+\xi)]A_2(s)N_J(s\tau)\,\mathrm{d}s+\frac{\tau}{2}\alpha_{0,2}+\frac{\mathrm{i}}{2\pi}\int_{\mathbb{R}}\mathrm{e}^{\mathrm{i}s(\tau+\xi)}\\&\times\left[\int_0^{\tau}sz[N_J(s\tau)N_K(sz)-N_J(sz)N_K(s\tau)]\,\mathrm{e}^{-\mathrm{i}sz}\hat{F}(z,s)\,\mathrm{d}z\right]\mathrm{d}s,\end{aligned} \tag{2.26}$$

in which

$$N_J(x)\equiv[J_0(x)-\mathrm{i}J_1(x)],\quad N_K(x)\equiv[K_0(-\mathrm{i}x)-K_1(-\mathrm{i}x)], \tag{2.27}$$

with $K_n(x)$ the modified Bessel function of the second kind and of the nth order; $\hat{F}(\tau,s)=\mathscr{F}(F(\tau,\cdot))(s)$; and $F(\tau,\xi)$ is obtained from (2.25) using (2.19). Higher-order contributions exhibit solutions that have the same structure as (2.26). In §A.1 of the Appendix the regularity of (2.26) at the shoreline is proved.

2.3. *Assigning the boundary value*

From (2.10) it is clear that two initial conditions, the first concerning $\phi|_{t=y}$ and the second concerning $\phi_t|_{t=y}$, have to be satisfied. However, at each order in ϵ, we can assign only one datum, since we have only one unknown function ($A_1(s)$ and $A_2(s)$ for the first and the second order respectively). This is a seeming contradiction. In fact, the initial condition on $\phi_t|_{t=y}$ is actually unknown, since as underlined in §2.1, β_0 has to be regarded as function of α_0. This implies that $\phi_t|_{t=y}$ is actually a result of our problem and cannot be regarded as a datum. (In §A.1.2 of the Appendix we show that the BVP with no condition on ϕ_t is ill posed.) After agreeing that we have to assign only one datum, i.e. $\phi|_{t=y}$, we pose

$$\phi|_{t=y} = -1 = \phi^{(0)}|_{t=y} + \epsilon\phi^{(1)}|_{t=y} + \epsilon^2\phi^{(2)}|_{t=y} + O(\epsilon^3). \tag{2.28}$$

We briefly recall that the condition $\phi = -1$ at $t = y$ corresponds to the assumption that the incoming characteristic curves start travelling inside the sloping region at the position $x = -1$ which, therefore, represents the seaward boundary of the domain. Since $\phi^{(0)}|_{t=y} = -1$, we obtain $\phi^{(n)}|_{t=y} = 0$ for $n \geqslant 1$. It is more convenient to assign the datum in the (τ, ξ)-space; in this case $t = y$ corresponds to $\tau = -2$. From (2.23) we get

$$A_1(s) = \frac{\mathscr{F}(\alpha_{0,1})\exp(2\,\mathrm{i}s)}{J_0(2s) + \mathrm{i}J_1(2s)}, \tag{2.29}$$

and from (2.26) we get the value of $A_2(s)$,

$$\begin{aligned} A_2(s) = {} & \frac{\mathscr{F}(\alpha_{0,2})\exp(2\,\mathrm{i}s)}{J_0(2s) + \mathrm{i}J_1(2s)} + \frac{\mathrm{i}s}{N_J(-2s)}\int_{-2}^{0} z[N_J(-2s)N_K(sz) \\ & - N_J(sz)N_K(-2s)]\,\mathrm{e}^{-\mathrm{i}sz}\hat{F}(z, s)\,\mathrm{d}z. \end{aligned}$$

Then, we obtain the following solution at the first order:

$$\phi^{(1)}(\tau, \xi) = \frac{1}{2\pi}\int_{\mathbb{R}} \mathrm{e}^{\mathrm{i}s(\tau+\xi+2)}\mathscr{F}(\alpha_{0,1})\frac{N_J(\tau s)}{N_J(-2s)}\,\mathrm{d}s + \frac{\tau}{2}\alpha_{0,1}. \tag{2.30}$$

And at the second order we have,

$$\begin{aligned} \phi^{(2)}(\tau, \xi) = {} & \frac{1}{2\pi}\int_{\mathbb{R}} \mathrm{e}^{\mathrm{i}s(\tau+\xi+2)}\mathscr{F}(\alpha_{0,2})\frac{N_J(\tau s)}{N_J(-2s)}\,\mathrm{d}s + \frac{\tau}{2}\alpha_{0,2} + \frac{\mathrm{i}}{2\pi}\int_{\mathbb{R}} s\,\mathrm{e}^{\mathrm{i}s(\tau+\xi)} \\ & \times \left[\frac{N_J(\tau s)}{N_J(-2s)}\int_{-2}^{0} z[N_J(-2s)N_K(sz) - N_J(sz)N_K(-2s)]\,\mathrm{e}^{-\mathrm{i}sz}\hat{F}(z, s)\,\mathrm{d}z\right. \\ & \left. + \int_{0}^{\tau} z\,[N_J(s\tau)N_K(sz) - N_J(sz)N_K(s\tau)]\;\mathrm{e}^{-\mathrm{i}sz}\hat{F}(z, s)\,\mathrm{d}z\right]\mathrm{d}s. \end{aligned}$$

The higher orders show solutions similar to the second-order solution. The graphical illustrations of the first-order solutions shown in figure 3 clearly highlight the solution structure and the regions of flattening and steepening (run-downs) as a function of the density of the characteristics.

3. Some results

In the following, some important results are illustrated, namely the approximate position of the shoreline and the explicit solution of the NSWEs up to the first and the second order. Such results have been obtained by extracting roots of equations using perturbation methods.

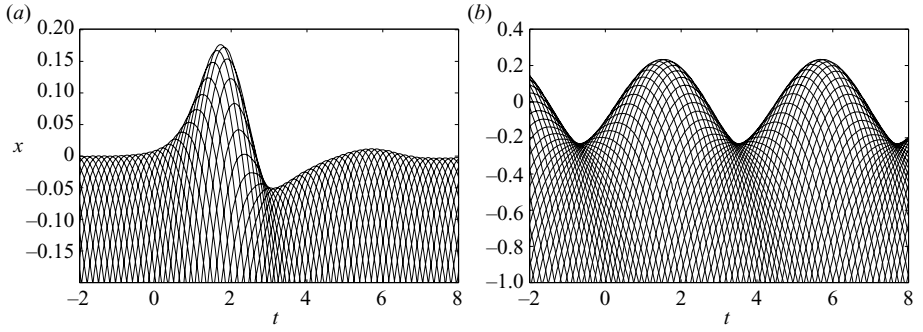

FIGURE 3. Paths of the first-order characteristic curves. (*a*) The solitary wave described in (3.21) ($\epsilon = 0.05$, $\gamma = 1.2$). (*b*) The periodic wave described in (3.23) ($\epsilon = 0.05$, $\omega = 1.5$).

3.1. *The shoreline equation*

In the (x, t)-space, the shoreline is made by an envelope of the characteristics. To obtain the equation representing such an envelope, we follow the procedure used by Whitham (1974) and consider two incoming curves which start at the initial times y and $y + dy$ and meet at time t and position $x = \phi$. Then we have

$$\phi(t, y + dy) = \phi(t, y) \quad \Rightarrow \quad \frac{\phi(t, y + dy) - \phi(t, y)}{dy} = 0. \tag{3.1}$$

Taking $dy \to 0$, we obtain

$$\phi_y(t, y) = 0, \tag{3.2}$$

which represents the equation of the envelope. The pairs (t, y) which satisfy (3.2) describe a curve in the (t, y)-plane. We, thus, assume that it is possible to get an explicit solution of the form $y = y(t)$ (the validity of such an assumption is studied in detail in §4). This function identifies, through y, the characteristic curve which reaches the shoreline at time t.

In the next section we find an explicit approximate expression for $y(t)$ by means of the usual perturbation method. For this reason we prefer to indicate the solution above by the symbol $y(t;\epsilon)$, highlighting the dependence on the perturbation parameter, ϵ. As a consequence of (3.2), such a solution has to satisfy

$$\phi_y(t, y)|_{y(t;\epsilon)} \equiv 0, \tag{3.3}$$

and because of its definition, it gives

$$x_s(t;\epsilon) = \phi(t, y)|_{y(t;\epsilon)}. \tag{3.4}$$

3.1.1. *Estimates of the shoreline position*

To find an explicit expression for the solution of the shoreline motion, we extend the perturbation method assuming $y(t;\epsilon)$ to have the following form:

$$y(t;\epsilon) = y_0(t) + \epsilon y_1(t) + \epsilon^2 y_2(t) + O(\epsilon^3). \tag{3.5}$$

Using a Taylor expansion, we get

$$\phi_y(t, y)|_{y(t;\epsilon)} = \phi_y^{(0)}(t, y_0) + \epsilon \left[\phi_{yy}^{(0)}(t, y_0)y_1 + \phi_y^{(1)}(t, y_0)\right] + \epsilon^2\Bigg[\phi_{yyy}^{(0)}(t, y_0)\frac{y_1^2}{2} + \phi_{yy}^{(0)}(t, y_0)y_2 + \phi_{yy}^{(1)}(t, y_0)y_1 + \phi_y^{(2)}(y, y_0)\Bigg] + O(\epsilon^3).$$

Imposing $\phi_y = 0$ (i.e. requiring each order of the expansion to be zero), we obtain

$$y_0(t) = t - 2, \quad y_1(t) = 2\phi_y^{(1)}(t, y_0), \quad y_2(t) = 2\left[y_1\phi_{yy}^{(1)}(t, y_0) + \phi_y^{(2)}(t, y_0)\right].$$

Knowledge of $y_0(t)$, $y_1(t)$ and $y_2(t)$ makes it possible to compute the shoreline position up to the second order of approximation. Its expression is given by the following expansion:

$$\phi(t, y)|_{y(t;\epsilon)} = \phi^{(0)}(t, y_0) + \epsilon \left[\phi_y^{(0)}(t, y_0)y_1 + \phi^{(1)}(t, y_0)\right] + \epsilon^2 \times \left[\phi_{yy}^{(0)}(t, y_0)\frac{y_1^2}{2} + \phi_y^{(0)}(t, y_0)y_2 + \phi_y^{(1)}(t, y_0)y_1 + \phi^{(2)}(t, y_0)\right] + O(\epsilon^3).$$

Hereinafter we use the following notation for the approximate shoreline:

$$\phi(t, y)|_{y(t;\epsilon)} = x_s(t;\epsilon) = \epsilon x_s^{(1)}(t) + \epsilon^2 x_s^{(2)}(t) + O(\epsilon^3), \tag{3.6}$$

in which

$$x_s^{(1)}(t) = \phi^{(1)}(t, y_0), \quad x_s^{(2)}(t) = \left[\frac{y_1^2}{4} + \phi^{(2)}(t, y_0)\right]. \tag{3.7}$$

Actually, it is possible to obtain a solution for x_s which is more accurate than a pure first-order solely using the first-order assignment. Using the definition of $y(t;\epsilon)$, we define the following 'first-half-order' solution for the shoreline:

$$x_s(t;\epsilon) = \epsilon x_s^{(1h)}(t) + O(\epsilon^2), \quad \text{where} \quad x_s^{(1h)}(t) = \phi^{(1)}(t, y_0 + \epsilon y_1). \tag{3.8}$$

Since $y_1(t) = \phi_y^{(1)}(t, y_0)$, $x_s^{(1h)}$ depends only on the first-order assignment, and thus, it is simpler than the second-order solution but more accurate than a pure first-order one.

3.2. *Assigning data on η and u*

The primary variables η and u at the seaward boundary of the domain are generally available from measurements. Then, the main problem is how to treat two seaward data, while on the contrary, the BVP requires only one datum (that is α_0). Since η and u are functions of both α_0 and β_0, it is not possible to assign η and u separately, but it is necessary to first extract α_0 and then solve the BVP through it. This procedure ensures that the analytical solution and the boundary data contain the same value of α_0. However, since the NSWEs are an approximate model of the real physical wave propagation, we cannot expect the same for the outgoing signal, that is β_0. Then, we have to assume that the analytical solution at the seaward boundary is in principle different from the seaward data obtained from measurements. For this reason, in the following we denote the solutions of the BVP at the seaward boundary by $\hat{\eta}$ and $\hat{u}$ in order to distinguish them from the boundary data η and u. Both pairs must contain the same value of α_0 but can, in principle, contain different outgoing signals, $\hat{\beta}_0$ and β_0 respectively. After the BVP is solved, $\hat{\beta}_0$ is found by imposing it to satisfy

the second boundary condition, that is the condition on $\phi_t|_{t=y}$. In fact, the second boundary condition always holds true notwithstanding it cannot be used until the BVP is solved (here we briefly recall that the value of $\phi_t|_{t=y}$ is a result of the solution procedure). Comparisons between the pairs $(\hat{\eta}, \hat{u})$ and (η, u) shall help understand the validity of the NSWEs.

Now, let us suppose the data to be small and, thus, have $\eta = \epsilon\eta_0$ and $u = \epsilon u_0$ with η_0, u_0 the functions of y. Then we calculate α_0 from the data and expand it in series of ϵ:

$$\alpha_0 = 2\sqrt{1+\epsilon\eta_0} + \epsilon u_0 + y = (2+y) + \epsilon(u_0+\eta_0) - \epsilon^2\frac{\eta_0^2}{4} + O(\epsilon^3). \tag{3.9}$$

This provides $\alpha_{0,0}, \alpha_{0,1}, \alpha_{0,2}$ and allows us to solve the problem. In the same way, we can obtain β_0 and then $\beta_{0,0}, \beta_{0,1}, \beta_{0,2}$, but generally, these values differ from the solution of the BVP. As a consequence, we use the variables $\hat{\eta}$, $\hat{u}$ and assume the following expansion in powers of ϵ:

$$\hat{\eta} = \epsilon\hat{\eta}_0 + \epsilon^2\hat{\eta}_1 + O(\epsilon^3), \quad \hat{u} = \epsilon\hat{u}_0 + \epsilon^2\hat{u}_1 + O(\epsilon^3). \tag{3.10}$$

Then, the expression of α_0 obtained through $\hat{\eta}$ and $\hat{u}$ is

$$\hat{\alpha}_0 = 2\sqrt{1+\hat{\eta}} + \hat{u} + y = (2+y) + \epsilon(\hat{\eta}_0+\hat{u}_0) + \epsilon^2\left(\hat{\eta}_1 - \frac{\hat{\eta}_0^2}{4} + \hat{u}_1\right) + O(\epsilon^3).$$

Considering the different ϵ-orders of the previous expression, we obtain $\hat{\alpha}_{0,0}, \hat{\alpha}_{0,1}, \hat{\alpha}_{0,2}$. The same procedure provides the unknown function $\hat{\beta}_0$ and then $\hat{\beta}_{0,0}, \hat{\beta}_{0,1}, \hat{\beta}_{0,2}$:

$$\hat{\beta}_0 = 2\sqrt{1+\hat{\eta}} - \hat{u} - y = (2-y) + \epsilon(\hat{\eta}_0-\hat{u}_0) + \epsilon^2\left(\hat{\eta}_1 - \frac{\hat{\eta}_0^2}{4} - \hat{u}_1\right) + O(\epsilon^3).$$

Finally, $\hat{\eta}$ and $\hat{u}$ can be evaluated solving the equations

$$\hat{\alpha}_{0,n} = \alpha_{0,n}, \quad \forall n \geqslant 1, \tag{3.11}$$

and imposing $\hat{\beta}_0$ to satisfy the second initial condition,

$$\phi_t|_{t=y} = \frac{3\hat{\alpha}_0 - \hat{\beta}_0}{4} - y, \tag{3.12}$$

at each order of ϵ. Using the expansions for $\hat{\alpha}_0$, $\hat{\beta}_0$ and, then, (3.11), we get

$$\frac{3\hat{\alpha}_0 - \hat{\beta}_0}{4} - y = 1 + \epsilon\left(\hat{u}_0 + \frac{\hat{\eta}_0}{2}\right) + O(\epsilon^2) = 1 + \epsilon\left(\alpha_{0,1} - \frac{\hat{\eta}_0}{2}\right) + O(\epsilon^2). \tag{3.13}$$

In the same way, using (2.16), we find

$$\phi_t|_{t=y} = 1 + \epsilon\phi_t^{(1)}|_{t=y} + O(\epsilon^2), \tag{3.14}$$

and comparing (3.13) and (3.14), we obtain the following first-order relation:

$$\phi_t^{(1)}|_{t=y} = \alpha_{0,1} - \frac{\hat{\eta}_0}{2}, \quad \Rightarrow \quad \hat{\eta}_0 = 2\left[\alpha_{0,1} - \phi_t^{(1)}|_{t=y}\right]. \tag{3.15}$$

At this stage, we just have to evaluate $\phi_t^{(1)}|_{t=y}$ from the first-order solution. Since $\partial/\partial\tau = \partial/\partial t$, we can take the τ-derivative of (2.30), obtaining

$$\phi_\tau^{(1)}(\tau,\xi) = \frac{\mathrm{i}}{2\pi}\int_{\mathbb{R}} \mathrm{e}^{\mathrm{i}s(\tau+\xi+2)}\frac{\mathscr{F}(\alpha_{0,1})}{J_0(2s)+\mathrm{i}J_1(2s)}\frac{J_1(s\tau)}{\tau}\,\mathrm{d}s + \frac{\alpha_{0,1}}{2}. \tag{3.16}$$

Since $t = y$ is equivalent to $\tau = -2$, we immediately obtain

$$\phi_t^{(1)}|_{t=y} \equiv \phi_\tau^{(1)}(-2, \xi) = \frac{\mathrm{i}}{4\pi} \int_{\mathbb{R}} \mathrm{e}^{\mathrm{i}s\xi} \mathscr{F}(\alpha_{0,1}) \frac{J_1(2s)}{J_0(2s) + \mathrm{i}J_1(2s)} \,\mathrm{d}s + \frac{\alpha_{0,1}}{2}.$$

Finally, using (3.15), we get

$$\hat{\eta}_0 = \frac{1}{2\pi} \int_{\mathbb{R}} \mathrm{e}^{\mathrm{i}sy} \mathscr{F}(\alpha_{0,1}) \frac{J_0(2s)}{J_0(2s) + \mathrm{i}J_1(2s)} \,\mathrm{d}s, \tag{3.17a}$$

$$\hat{u}_0 = \frac{1}{2\pi} \int_{\mathbb{R}} \mathrm{e}^{\mathrm{i}sy} \mathscr{F}(\alpha_{0,1}) \frac{\mathrm{i}J_1(2s)}{J_0(2s) + \mathrm{i}J_1(2s)} \mathrm{d}s. \tag{3.17b}$$

We cannot obtain a representation of $\alpha_{0,1}$ as function of $\hat{\eta}_0$ or $\hat{u}_0$ from (3.17*a*) and (3.17*b*): in both cases we would get integrals with singular kernels. For example, using (3.17*a*), we can try to rewrite $\alpha_{0,1}$ as function of η_0. We get

$$\alpha_{0,1} = \frac{1}{2\pi} \int_{\mathbb{R}} \mathrm{e}^{\mathrm{i}sy} \mathscr{F}(\hat{\eta}_0) \left(1 + \mathrm{i}\frac{J_1(2s)}{J_0(2s)}\right) \,\mathrm{d}s. \tag{3.18}$$

Since $J_0(2s) = 0$ on a infinite set of points and goes to zero as s^{-1}, such an integral is unbounded. The same result is obtained for $\hat{u}$. Finally, this confirms that α is the correct conservative variable.

Now we can use (3.7) to evaluate the shoreline up to the first order. Since $y_0 = t - 2$ corresponds to $\tau = 0$, we have

$$x_s(t;\epsilon) = \epsilon x_s^{(1)}(t) + O(\epsilon^2) = \frac{\epsilon}{2\pi} \int_{\mathbb{R}} \mathrm{e}^{\mathrm{i}st} \frac{\mathscr{F}(\alpha_{0,1})}{N_J(-2s)} \,\mathrm{d}s + O(\epsilon^2). \tag{3.19}$$

3.3. *Some examples*

Classical wave examples, namely periodic waves and the solitary wave, are discussed in the following. In order to assign proper data at the seaward boundary, we use the results obtained through the Korteweg–de Vries (KdV) equations. Indeed, since the α datum is naturally associated with the incoming component of waves, we can assume it to be related to waves of permanent shape moving from the constant-depth region inside the sloping region. In this case the KdV equations give $\eta_0 = u_0$ at the first order of approximation (see Mei 1983), and using (3.9), we get $\alpha_{0,1} = 2\eta_0$. In the following we write $\eta_0 = \eta_0^I$ and $u_0 = u_0^I$ to underline that these data are associated with the incoming waves. These are the only assumptions under which we can express α as a function of η. Solutions $\hat{\eta}_0$ and $\hat{u}_0$ at the seaward boundary are, generally, different from η_0 and u_0, since they also account for the wave reflection at the shoreline. However, we can obtain the reflected-wave component at the seaward boundary simply defining $\eta_0^R = \hat{\eta}_0 - \eta_0^I$ and $u_0^R = \hat{u}_0 - u_0^I$. Using the previous definition it is also simple to prove the relations

$$\eta_0^R + u_0^R = 0, \quad \eta_0^R - u_0^R = \hat{\beta}_{0,1}, \tag{3.20}$$

which confirms that $\hat{\beta}$ is associated with the reflection of waves at the shoreline.

3.3.1. *The solitary wave*

We study the run-up of a solitary wave by means of the well-known case studied by Synolakis (1987). Using the solution of the KdV equations and adapting it to the scaling at hand, we obtain

$$\eta_0^I(y) = \mathrm{sech}^2(\gamma y) \quad \text{with} \quad \gamma = \frac{\sqrt{3\epsilon}}{2\tan(\theta)}. \tag{3.21}$$

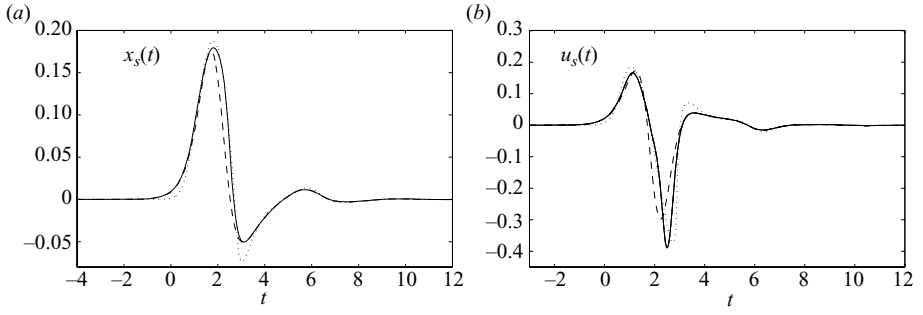

FIGURE 4. Solitary wave solution at the shoreline for $\epsilon = 0.05$ and $\gamma = 1.2$: (*a*) $x_s(t)$ and (*b*) $u_s(t)$ at the first order (dashed lines), at the first-half-order (solid lines) and the second-order solution of Antuono & Brocchini (2007; dotted lines).

From Synolakis (1987), we also get

$$\mathscr{F}(\alpha_{0,1})(s) = \mathscr{F}\left(2\eta_0^I\right)(s) = \frac{2\pi}{\gamma^2} s \operatorname{csch}\left(\frac{\pi}{2\gamma} s\right). \tag{3.22}$$

Since ϵ and $\tan(\theta)$ are independent, γ and ϵ are independent as well.

In the following we illustrate the model performances by plotting results which are a direct numerical evaluation of the asymptotic analytical solutions.

In figure 4 we show a comparison between the first-order and the first-half-order solution of the present model and the second-order solution of Antuono & Brocchini (2007) for the shoreline position and velocity and for $\epsilon = 0.05$ and $\gamma = 1.2$.

For the present model, the shoreline velocity is evaluated by using (1.5). We also recall that the solution of Antuono & Brocchini (2007) for the BVP is achieved by using the hodograph transformation of Carrier & Greenspan (1958). The difference between $x_s^{(1h)}$ and $x_s^{(1)}$ (recall 3.8) is small and $x_s^{(1h)}$ seems to better represent the nonlinear flow characteristics at the shoreline, that is more rounded run-ups and narrower run-downs. Moreover, the match of both present solutions with the second-order solution of Antuono & Brocchini (2007) is fairly good (apart from a region near the run-down). A larger discrepancy is observed between $u_s^{(1h)}$ and $u_s^{(1)}$, while the match between $u_s^{(1h)}$ and the second-order solution of Antuono & Brocchini (2007) displays an overall improvement. The maximum run-up generally appears two time units later than the $\alpha_{0,1}$ maximum value at the seaward boundary (compare figure 4 with figure 5*a*). This happens because the characteristic curves spend about two time units to travel from the seaward boundary up to the shoreline – this is also evident by inspection of the trivial solution ((2.13) and (2.14)).

A similar argument holds for the reflected signals η_0^R and u_0^R in figures 5(*e*) and 5(*f*) whose maxima at the seaward limit appear four time units later than the $\alpha_{0,1}$ maximum value. Finally, it is interesting to note the excellent match between $\hat{\eta}_0$ and η_0^I and between $\hat{u}_0$ and u_0^I during the earliest instants. This is physically meaningful, since at the earliest instants there is no reflection from the shoreline, and therefore, the incoming data have to coincide with the solution. Moreover, this confirms our initial assumption, $\eta_0^I = u_0^I$, deduced from the KdV solution. Figures 5(*c*) and 5(*d*) also clearly illustrate the superposition of the incoming and reflected components of $\hat{\eta}_0$ and $\hat{u}_0$ at the seaward boundary. This exact (at the chosen order of approximation) analysis of wave (incoming and reflected) interaction at the seaward boundary of the

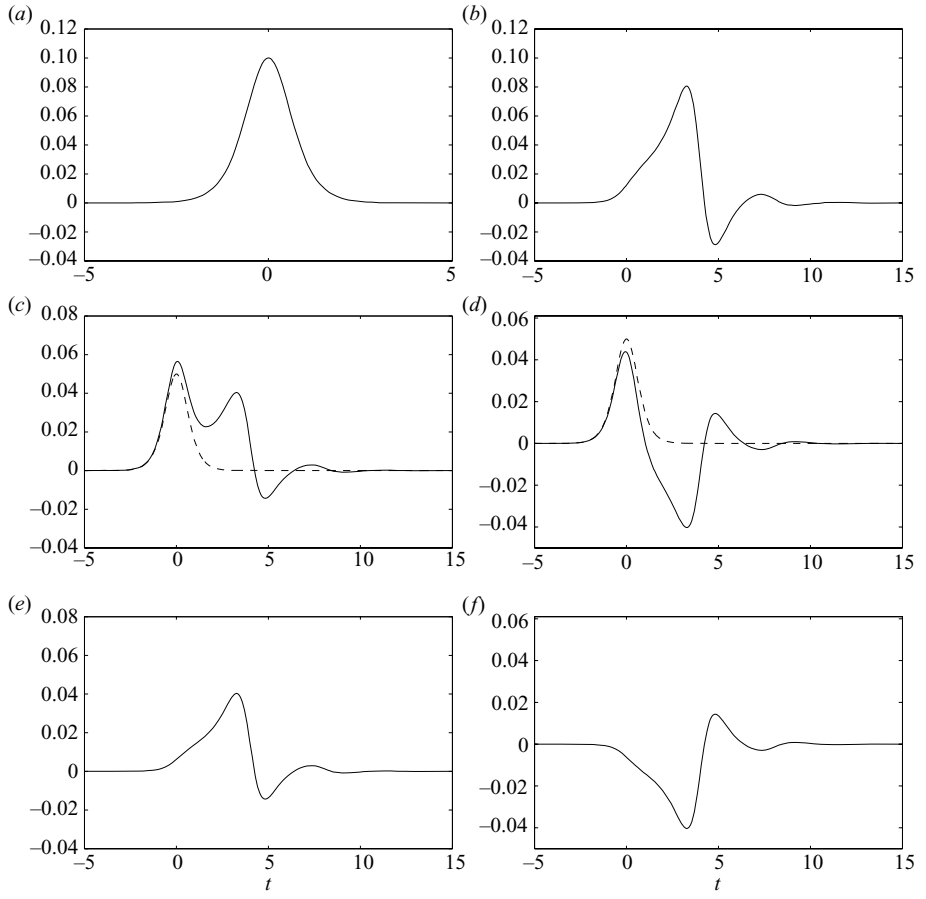

FIGURE 5. Solitary wave solution at the seaward boundary for $\epsilon = 0.05$ and $\gamma = 1.2$: (*a*) $\epsilon\alpha_0$; (*b*) $\epsilon\beta_0$; (*c*) $\epsilon\hat{\eta}_0$ (solid line) and $\epsilon\eta_0^I$ (dashed line); (*d*) $\epsilon\hat{u}_0$ (solid line) and ϵu_0^I (dashed line); (*e*) $\epsilon\eta_0^R$; (*f*) ϵu_0^R.

domain is only possible by virtue of the fact that we have solved a BVP rather than an initial value problem.

Notwithstanding the fact that the assumption $\eta_0^I = u_0^I$ is exact only in the case of travelling waves of permanent shape, it proves to be good also for waves of generic shape entering the sloping region. This is due to the fact that at the seaward boundary we may treat wave propagation as linear. In the following, we apply such an assumption to periodic waves.

3.3.2. *Periodic waves*

Let us consider the following periodic datum:

$$\eta_0^I(y) = \cos(\omega y). \tag{3.23}$$

In this special case, we can obtain an explicit solution for $\phi^{(1)}$ (see Appendix B).

In figure 6 we show the first-order and the first-half-order shoreline position and velocity solutions as predicted by the present model and the second-order solutions of the model of Antuono & Brocchini (2007) for $\epsilon = 0.05$ and $\omega = 1.5$.

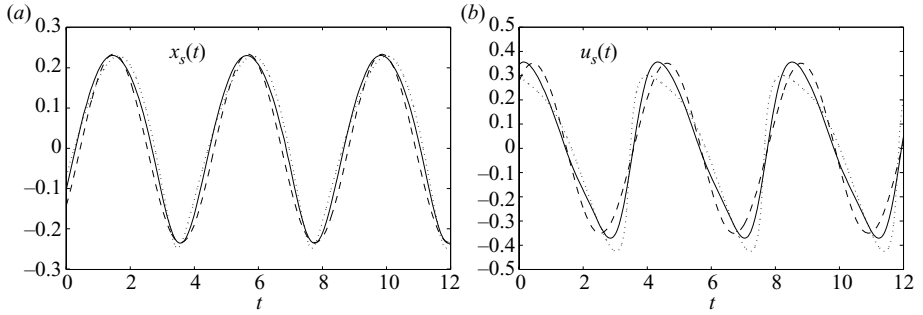

FIGURE 6. Periodic wave solution at the shoreline for $\epsilon = 0.05$ and $\omega = 1.5$: (*a*) $x_s(t)$ and (*b*) $u_s(t)$ at the first order (dashed lines) and at the first half-order (solid lines), and the second-order solution of Antuono & Brocchini (2007) (dotted lines).

For what concerns the shoreline position, apart from the first-order solution, nonlinear effects are evident and are characterized by rounded run-ups and narrow run-downs. However, differences among the solutions are small, with $x_s^{(1h)}$ better reproducing the second-order solution of Antuono & Brocchini (2007) than $x_s^{(1)}$.

On the contrary, larger discrepancies are observed for the shoreline velocity, since nonlinearities act more strongly and force a significant skewness (steepening) of the velocity signals associated with the present solution $u_s^{(1h)}$ and with the second-order solution of Antuono & Brocchini (2007). This behaviour contrasts with that of the shoreline solution, especially with the first-order one which is represented by a simple sinusoidal wave.

Actually, this is also the case for the solution at the seaward boundary of the domain. (The outputs illustrating the direct numerical evaluation of the asymptotic solutions are shown in figure 7.) However, this does not mean that the first-order solution is equivalent to the solution of the linear shallow-water equations.

In the following we prove that the present model preserves the nonlinear features of the propagation phenomenon, so that it is not possible to represent the first-order solution as a simple sinusoidal wave in the whole domain.

3.4. *Evaluation of* $u(x,t)$ *and* $\eta(x,t)$

Once the approximate characteristic curves have been obtained, we can evaluate u and η as functions of x and t, obtaining a nonlinear approximate solution of the BVP for the NSWEs. To do this, we first need to know the incoming and outgoing characteristic curves crossing a generic point (x,t) of the domain. Once they are known, we can get the associated Riemann invariants $\alpha(x,t)$ and $\beta(x,t)$ and, finally, the solutions $u(x,t)$ and $\eta(x,t)$ simply using (1.4).

We start by looking for the characteristic curves crossing a generic (x,t)-point, where $x = \phi(t,y)$. Therefore, to express all the quantities as functions of x and t, we first need to make y explicit. In this way we get $y = \tilde{y}(x,t)$ which represents the time at which the characteristic curve reaching (x,t) starts travelling inside the domain. Actually, since the point (x,t) is reached by an incoming and an outgoing characteristic curve, we expect to find two different functions $\tilde{y}^{(+)}(x,t)$ and $\tilde{y}^{(-)}(x,t)$

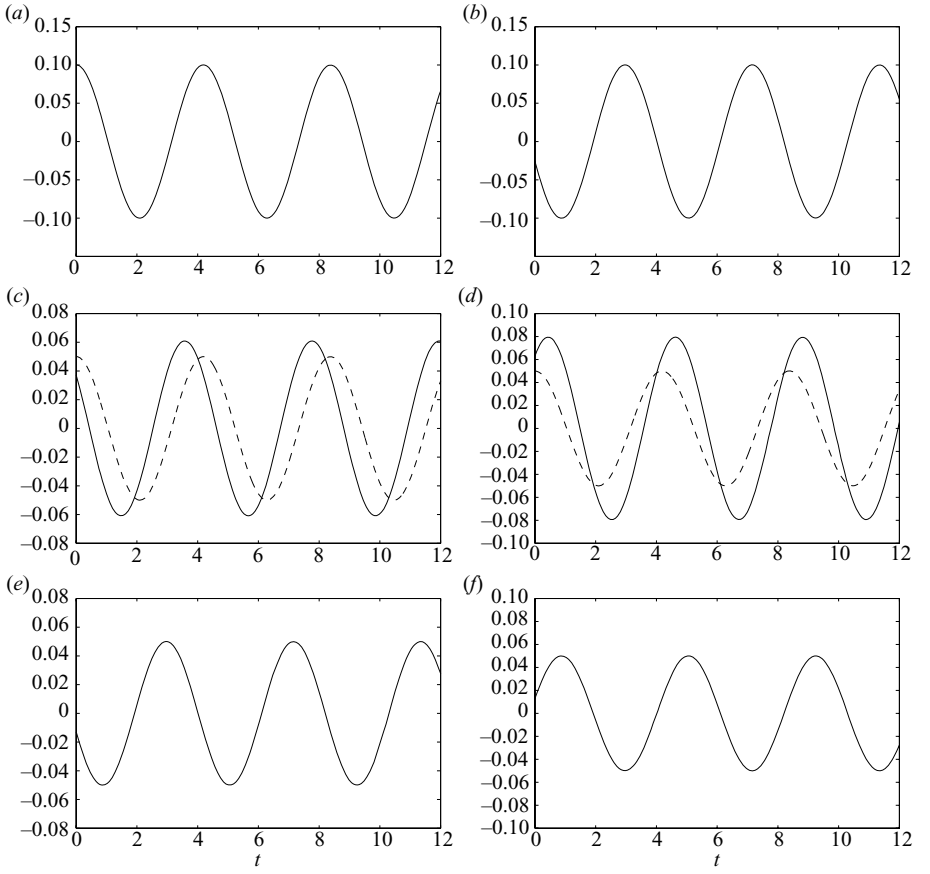

FIGURE 7. Periodic wave solution at the seaward boundary for $\epsilon = 0.05$ and $\omega = 1.5$: (*a*) $\epsilon\alpha_0$; (*b*) $\epsilon\beta_0$; (*c*) $\epsilon\hat{\eta}_0$ (solid line) and $\epsilon\eta_0^I$ (dashed line); (*d*) $\epsilon\hat{u}_0$ (solid line) and ϵu_0^I (dashed line); (*e*) $\epsilon\eta_0^R$; (*f*) ϵu_0^R.

(see figure 8). Using the solution up to the second order, we have

$$x = -\frac{(t-y-2)^2}{4} + \epsilon\phi^{(1)}(t,y) + \epsilon^2\phi^{(2)}(t,y) + O(\epsilon^3). \tag{3.24}$$

A first attempt to get $\tilde{y}$ is to assume the usual expansion $\tilde{y}(x,t) = \tilde{y}_0(x,t) + \epsilon\tilde{y}_1(x,t) + \epsilon^2\tilde{y}_2(x,t) + O(\epsilon^3)$. Unfortunately, this gives a solution which is not uniform, that is which fails in the evaluation of $u(x,t)$ and $\eta(x,t)$ for $x > 0$. To overcome the problem, we must consider an expansion compatible with the presence of the moving shoreline $x_s(t)$. Then, we assume the following second-order perturbation expansion for $\tilde{y}$:

$$\tilde{y}(x,t) = (t-2) \pm 2\sqrt{-x + \epsilon x_s^{(1)} + \epsilon^2 x_s^{(2)} + O(\epsilon^3)} + \epsilon\tilde{y}_1 + \epsilon^2\tilde{y}_2 + O(\epsilon^3). \tag{3.25}$$

Stopping at the second-order approximation, $\tilde{y}(x,t)$ is defined for $x \leqslant x_s(t)$, the higher orders being defined by adding further terms of $x_s(t)$ inside the square root and more unknown functions $\tilde{y}_n$. Moreover, using the expansion in (3.25), the structure of the two roots $\tilde{y}^{(+)}(x,t)$ and $\tilde{y}^{(-)}(x,t)$ is immediately clear. For the sake of brevity, we indicate the square root in (3.25) simply through $S(x,t)$. Then, substituting (3.25) in

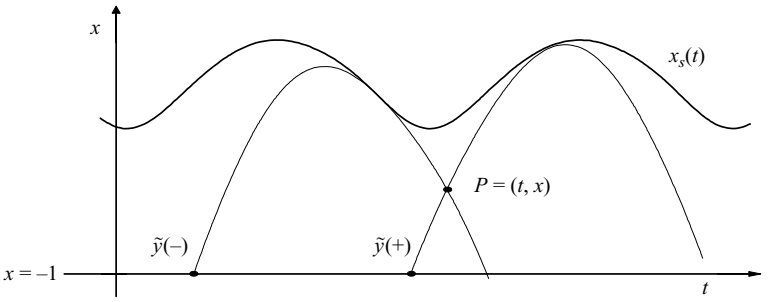

FIGURE 8. Sketch of the problem discussed in §3.4. The figure represents the shoreline position and two different characteristic curves crossing at the generic point $P=(t,x)$ for the periodic wave described in (3.23) with $\epsilon=0.05$ and $\omega=1.5$.

(3.24), we get

$$\tilde{y}_1^{(\pm)} = \pm\frac{\phi^{(1)}\left(t,\tilde{y}_0^{(\pm)}\right)-x_s^{(1)}}{S(x,t)},$$
$$\tilde{y}_2^{(\pm)} = \pm\frac{1}{S(x,t)}\left[-\frac{\left(\tilde{y}_1^{(\pm)}\right)^2}{4}+\tilde{y}_1^{(\pm)}\phi_y^{(1)}\left(t,\tilde{y}_0^{(\pm)}\right)+\phi^{(2)}\left(t,\tilde{y}_0^{(\pm)}\right)-x_s^{(2)}\right],$$

in which $\tilde{y}_0^{(\pm)}=(t-2)\pm 2S(x,t)$. As proof of the coherence of the previous approach, we note that for $x\to x_s(t)$, i.e. for $S(x,t)\to 0$, we have

$$\tilde{y}_0^{(\pm)}(x,t)\to y_0(t),\quad \tilde{y}_1^{(\pm)}(x,t)\to y_1(t),\quad \tilde{y}_2^{(\pm)}(x,t)\to y_2(t). \tag{3.26}$$

The first root ($\tilde{y}^{(+)}$) is associated with the incoming characteristic curve carrying the value $\alpha(\tilde{y}^{(+)})$, the latter with the outgoing characteristic curve carrying the value $\beta(\tilde{y}^{(-)})\equiv-\alpha(\tilde{y}^{(-)})$. These are the incoming and outgoing characteristic curves crossing the point (x,t), and therefore, using (1.4), we obtain $u(x,t)$ and $\eta(x,t)$. Since the two roots coincide for $x\to x_s(t)$ ($\tilde{y}^{(+)}=\tilde{y}^{(-)}\equiv\tilde{y}_s$), we simply obtain $\alpha(\tilde{y}_s)=-\beta(\tilde{y}_s)$, which is consistent with the shoreline definition ($c=0\Leftrightarrow\alpha=-\beta$).

Finally, we observe that even if the characteristic path only partially preserves its nonlinear nature, the construction of explicit solutions as a function of the dependent variables u and η is a fully nonlinear process. This means that the approximation of the characteristic path does not correspond to a naïve linearization of the NSWEs.

We can now use the previous results to get the solutions $\eta(x,t)$ and $u(x,t)$ all over the domain. At the first order of approximation in ϵ it is

$$\alpha(x,t)=\left(2+\tilde{y}_0^{(+)}\right)+\epsilon\left[\alpha_{0,1}\left(\tilde{y}_0^{(+)}\right)+\tilde{y}_1^{(+)}\right]+O(\epsilon^2), \tag{3.27}$$
$$\beta(x,t)=-\left(2+\tilde{y}_0^{(-)}\right)-\epsilon\left[\alpha_{0,1}\left(\tilde{y}_0^{(-)}\right)+\tilde{y}_1^{(-)}\right]+O(\epsilon^2). \tag{3.28}$$

Then using (1.4), we obtain

$$\eta(x,t)=\epsilon\left\{x_s^{(1)}(t)+\frac{S(x,t)}{2}\left[\alpha_{0,1}\left(\tilde{y}_0^{(+)}\right)-\alpha_{0,1}\left(\tilde{y}_0^{(-)}\right)+\tilde{y}_1^{(+)}-\tilde{y}_1^{(-)}\right]\right\}$$
$$+\frac{\epsilon^2}{16}\left[\alpha_{0,1}\left(\tilde{y}_0^{(+)}\right)-\alpha_{0,1}\left(\tilde{y}_0^{(-)}\right)+\tilde{y}_1^{(+)}-\tilde{y}_1^{(-)}\right]^2 \tag{3.29}$$

and

$$u(x,t)=\frac{\epsilon}{2}\left[\alpha_{0,1}\left(\tilde{y}_0^{(+)}\right)+\alpha_{0,1}\left(\tilde{y}_0^{(-)}\right)+\tilde{y}_1^{(+)}+\tilde{y}_1^{(-)}\right]+O(\epsilon^2). \tag{3.30}$$

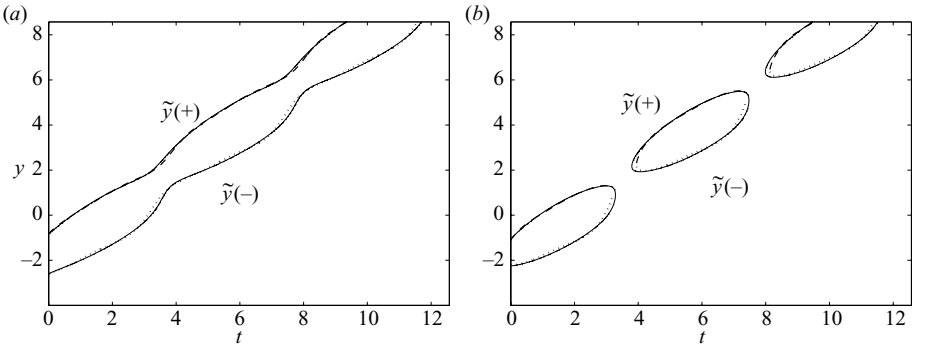

FIGURE 9. Contour lines $\phi(t, y) = x$ (solid lines), $\tilde{y}^{(+)}(x, t)$ (dot-dashed line) and $\tilde{y}^{(-)}(x, t)$ (dotted line) for the periodic datum in (3.23) with $\epsilon = 0.05$ and $\omega = 1.5$: (*a*) $x = -0.3$, (*b*) $x = -0.2$.

We can also obtain the expression of the onshore velocity at the shoreline, u_s. At the shoreline, we have

$$\tilde{y}_0 \equiv y_0 = t - 2, \quad \tilde{y}_s = y_0 + 2\epsilon\phi_y^{(1)}(t, y_0) + O(\epsilon^2), \tag{3.31}$$

and then, we can also evaluate α at the shoreline:

$$\alpha_s \equiv \alpha(\tilde{y}_s) = t + \epsilon\left[2\phi_y^{(1)}(t, y_0) + \alpha_{0,1}(y_0)\right] + O(\epsilon^2). \tag{3.32}$$

Since $\alpha_s = -\beta_s$ and, thus, $u_s = \alpha_s - t$, we, finally, obtain

$$u_s(t) = \epsilon\left[2\phi_y^{(1)}(t, y_0) + \alpha_{0,1}(y_0)\right] + O(\epsilon^2) = \epsilon u_s^{(1)} + O(\epsilon^2). \tag{3.33}$$

It is also easy to show that at the first ϵ-order we have

$$u_s^{(1)} = \frac{\mathrm{d}x_s^{(1)}}{\mathrm{d}t}. \tag{3.34}$$

This result is consistent with the condition $\dot{x} = u$ which must hold along the shoreline.

In figure 9 we show a direct numerical evaluation of the contour lines of the first-order solution in (3.24) (solid lines) along with their first-order approximations, that is the curves $\tilde{y}^{(+)}(x, t)$ and $\tilde{y}^{(-)}(x, t)$ (dotted and dashed lines) at fixed values of x. It is evident that the comparison between them is excellent. It is understood that a real analytical solution exists if and only if $x \leqslant x_s(t)$. Conversely, during the time intervals in which $x > x_s(t)$, the analytical solution has complex values. This is obvious, since from a physical point of view, no water is found for $x > x_s(t)$. For these reasons, in figures 9 we show the solution of (3.24) for the periodic datum in (3.23) only during the instants for which $x \leqslant x_s(t)$. To produce figure 9(*a*) we have chosen $x = -0.3$. Since in this case $x < x_s(t)$, $\forall t \in \mathbb{R}$, a real analytical solution exists $\forall t \in \mathbb{R}$, and the numerical solution is represented by two distinct curves, the upper one being $\tilde{y}^{(+)}(x, t)$ and the lower one being $\tilde{y}^{(-)}(x, t)$. We recall that solutions $\tilde{y}^{(\pm)}(x, t)$ represent the starting instant at which the incoming and outgoing characteristic curves, crossing the (x, t)-point, enter the sloping region.

Figure 9(*b*) has been produced by using $x = -0.2$. In this case there are some time intervals for which $x_s(t) < x$, and therefore, the solution is not global; i.e. it is not defined, $\forall t \in \mathbb{R}$. As a consequence, the exact solution is represented by elliptic-type patterns, the upper parts being associated with $\tilde{y}^{(+)}(x, t)$ and the lower ones with $\tilde{y}^{(-)}(x, t)$.

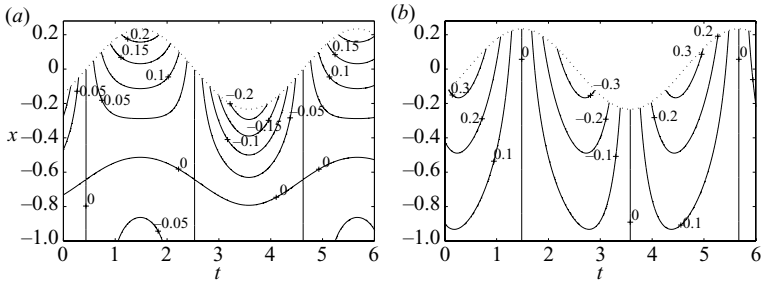

FIGURE 10. Contour lines of the first-order solutions for the periodic datum in (3.23) with $\epsilon = 0.05$ and $\omega = 1.5$: (*a*) $\eta(x,t)$, (*b*) $u(x,t)$.

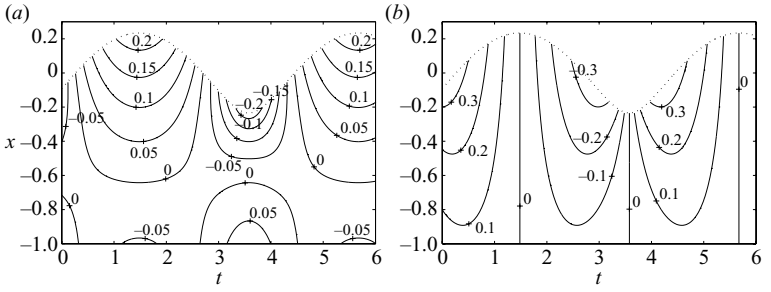

FIGURE 11. Contour lines of the first-order solutions obtained by using the hodograph model described in Antuono & Brocchini (2007) for the periodic datum in (3.23) with $\epsilon = 0.05$ and $\omega = 1.5$: (*a*) $\eta(x,t)$, (*b*) $u(x,t)$.

Finally, figures 10(*a*) and 10(*b*) show the contour lines of the solutions given in (3.29) and (3.30) for the periodic datum in (3.23) with $\epsilon = 0.05$ and $\omega = 1.5$. The typical cell-type structure for the solution of the 'beach problem' of the NSWEs forced by periodic waves and developing a standing wave pattern (Carrier & Greenspan 1958; Brocchini & Peregrine 1996) is here easily obtained from the first-order solution ((3.29) and (3.30)) with no need of any coordinate transformation. Cells, confined by surface contours of zero level, are characterized by the largest values near the shoreline, while an antisymmetric pattern characterizes the solution for the onshore velocity.

In order to compare the results above with the analytical solutions available in the literature, in figures 11(*a*) and 11(*b*) we draw the contour lines of the first-order solution obtained by using the hodograph model described in Antuono & Brocchini (2007). Note that such a solution coincides with the periodic solution found by Carrier & Greenspan (1958) when the latter is imposed to solve the BVP described in §3.2. The contour lines for $u(x,t)$ are almost identical in both cases (figures 10*b* and 11*b*), while on the contrary, some discrepancies arise for $\eta(x,t)$. This is due to the different ways in which the models account for the nonlinearities. Indeed, both the solutions for η retain some $O(\epsilon^2)$ contributions (see Antuono & Brocchini 2007).

Similarly, it is very simple to obtain the time evolution of the near-shoreline flow. Figure 12 shows some snapshots of $\eta(x,t)$ and $u(x,t)$ at different times during a complete swash cycle: the free-surface evolution is characterized by the classical nodal point characteristic of the standing wave pattern. (This benchmark is one of the most useful to assess the value of numerical solvers of the NSWEs with respect to

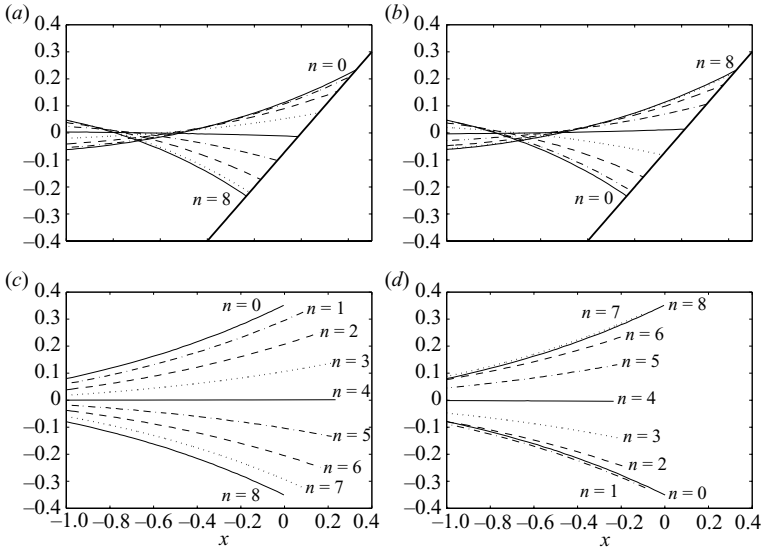

FIGURE 12. Snapshots of the first-order solutions for the periodic datum in (3.23) with $\epsilon = 0.05$ and $\omega = 1.5$: (*a*) $\eta(x,t)$ during the run-up to run-down phase ($t_n = t_0 + nT/16$); (*b*) $\eta(x,t)$ during the run-down to run-up phase ($t_n = t_0 + T/2 + nT/16$); (*c*) $u(x,t)$ from the maximum shoreward velocity to the maximum seaward velocity ($t_n = t_0 - T/4 + nT/16$); (*d*) $u(x,t)$ from the maximum seaward velocity to the maximum shoreward velocity ($t_n = t_0 + T/4 + nT/16$). For all panels $t_0 = 1.4834$, $T = 2\pi/\omega$ and $n = 0, 1, \ldots, 8$. The thick solid line is the beach bottom in (*a*) and (*b*).

the description of near-shoreline flows, e.g. Hubbard & Dodd 2002.). Using the first-order solution, it is simple to show that the maximum shoreward/seaward velocities lead the maximum run-ups/run-downs by $T/4$ (T is the wave period) and that they occur when $x_s(t) = 0$. For the sake of clarity, $\eta(x,t)$ has been plotted starting from the maximum run-up to the maximum run-down and vice versa. Similarly, $u(x,t)$ has been drawn starting from the maximum shoreward velocity to the maximum seaward velocity and vice versa. This implies that times for $\eta(x,t)$ and $u(x,t)$ are not the same (see also the figure caption).

Finally in figure 13 we show the comparison between some snapshots of $\eta(x,t)$ and $u(x,t)$ as computed through the present model and that of Antuono & Brocchini (2007). Although some discrepancies are observed (especially for $\eta(x,t)$), the global behaviour is fairly good and improves if we refer to the second-order solution (see figure 14). Since the structures of the hodograph solution and of the solution of the present model are completely different, the match between them is regarded to be good.

The procedure to get the second-order solution for the periodic case is the same as shown in Appendix B, even if the computations for the non-homogeneous part of the solution are rather long and tedious. The simplest way to obtain the second-order solution is to rewrite $\hat{F}(z,s)$ as

$$\hat{F}(z,s) = A(z)\delta(s-2\omega) + B(z)\delta(s) + C(z)\delta(s+2\omega), \tag{3.35}$$

where δ indicates the Dirac 'function'. (The expressions for $A(z)$, $B(z)$ and $C(z)$ can be easily obtained by using, for example, the software package Maple and then translating

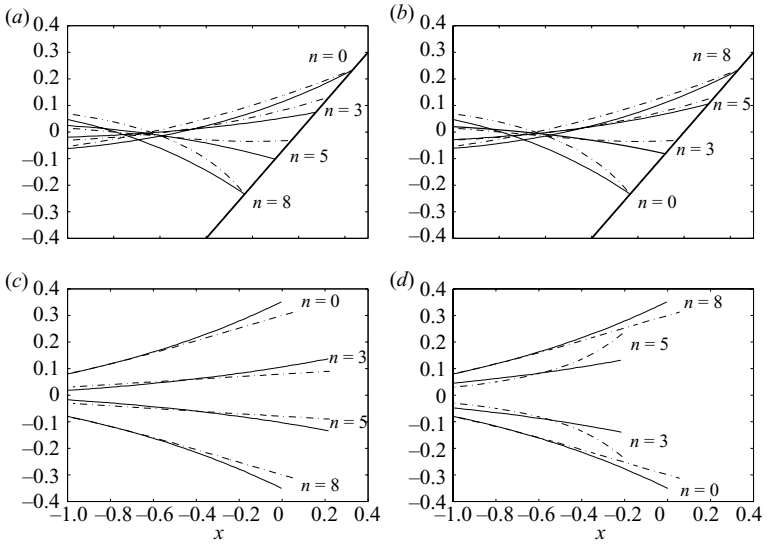

FIGURE 13. Comparison between the first-order solutions as obtained through the present model (solid lines) and the model of Antuono & Brocchini (2007; dot-dashed lines) for the periodic datum in (3.23) with $\epsilon = 0.05$ and $\omega = 1.5$. Time evolution of the flow variables is as reported in the caption of figure 12. For all panels $t_0 = 1.4834$, $T = 2\pi/\omega$ and $n = 0, 3, 5, 8$.

them into either a Fortran or Matlab code through the package 'CodeGeneration'.) The formulation in (3.35) enables an easy and straightforward evaluation of the main second-order contributions. Then, similar to (3.27) and (3.28), we get

$$\alpha(x,t) = 2 + \tilde{y}_0^{(+)} + \epsilon\left[\alpha_{0,1}\left(\tilde{y}_0^{(+)}\right) + \tilde{y}_1^{(+)}\right] + \epsilon^2\left[\tilde{y}_2^{(+)} + \tilde{y}_1^{(+)}\dot{\alpha}_{0,1}\left(\tilde{y}_0^{(+)}\right) + \alpha_{0,2}\left(\tilde{y}_0^{(+)}\right)\right],$$
$$\beta(x,t) = -2 - \tilde{y}_0^{(-)} - \epsilon\left[\alpha_{0,1}\left(\tilde{y}_0^{(-)}\right) + \tilde{y}_1^{(-)}\right] - \epsilon^2\left[\tilde{y}_2^{(-)} + \tilde{y}_1^{(-)}\dot{\alpha}_{0,1}\left(\tilde{y}_0^{(-)}\right) + \alpha_{0,2}\left(\tilde{y}_0^{(-)}\right)\right].$$

To close the section and illustrate even better the power of the present method, we study the evolution of the interaction of two waves within the domain in a similar manner as Brocchini & Peregrine (1996). Therefore, using wave parameters similar to those of figure 2 of Brocchini & Peregrine (1996), we analyse the following bimodal datum:

$$\alpha_{0,1}(y) = 2\epsilon\left[\cos(\omega_1 y) + \Delta\cos(\omega_2 y)\right]. \tag{3.36}$$

The first-order solution, $\phi^{(1)}$, is simply obtained as a linear superposition of two solutions of the type shown in (B 4): the first one with frequency ω_1 and the second one with frequency ω_2 and amplitude Δ. Notwithstanding that, the solutions for $\eta(x,t)$ and $u(x,t)$ are intrinsically nonlinear. Figure 15 shows the contour lines for $\eta(x,t)$ and $u(x,t)$, which illustrate the interaction of the mentioned modes.

The results found in the present section represent something new within the available literature. Indeed, for the first time it is possible to get an approximate nonlinear solution of the NSWEs over the entire domain of interest (i.e. including the interaction of wave fields) directly in the physical space without using characteristic variables. This removes the need for the numerical methods typically used to convert the hodograph variables into the physical ones and allows for a straightforward formulation of the BVP solution.

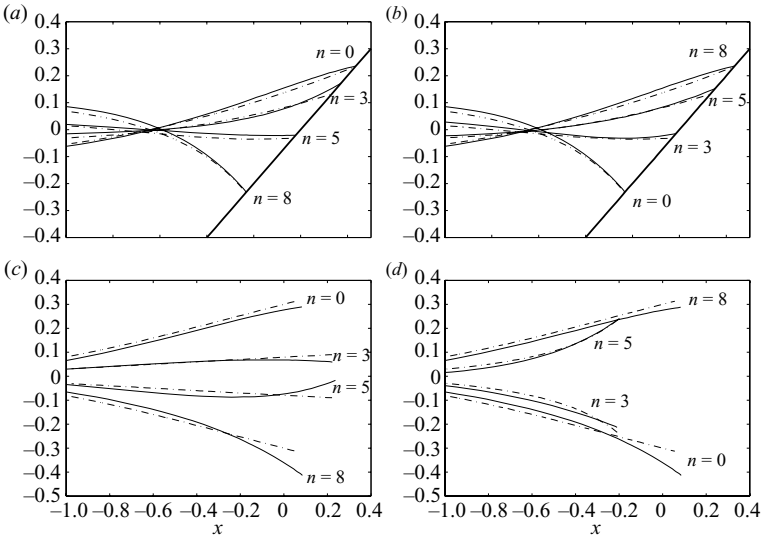

FIGURE 14. Comparison between the second-order solutions as obtained through the present model (solid lines) and the model of Antuono & Brocchini (2007; dot-dashed lines) for the periodic datum in (3.23) with $\epsilon = 0.05$ and $\omega = 1.5$. Time evolution of the flow variables is as reported in the caption of figure 12. For all panels $t_0 = 1.4834$, $T = 2\pi/\omega$ and $n = 0, 3, 5, 8$.

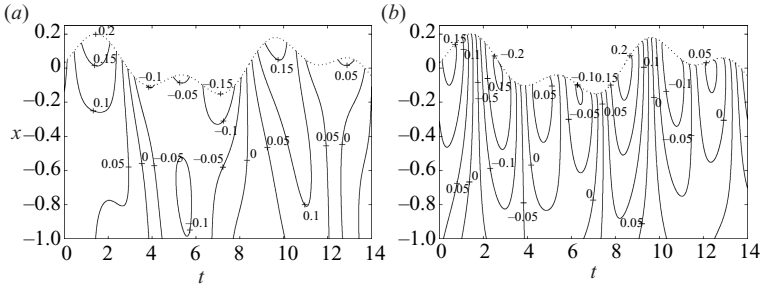

FIGURE 15. Contour lines of the first-order solutions for the bimodal periodic datum in (3.36) with $\epsilon = 0.05$, $\omega_1 = 2/3$, $\omega_2 = 1.6$ and $\Delta = 1/3$: (*a*) $\eta(x, t)$, (*b*) $u(x, t)$.

4. Breaking condition

We have already shown (§3.1) that equation $\phi_y = 0$ gives the shoreline position and have assumed that it was possible to get an explicit solution $y(t;\epsilon)$. However, this is not always possible. Indeed, on computing the t-derivative of (3.3), we get

$$\frac{\mathrm{d}y}{\mathrm{d}t}\phi_{yy}(t, y)|_{y(t;\epsilon)} + \phi_{yt}(t, y)|_{y(t;\epsilon)} = 0. \tag{4.1}$$

It is, therefore, evident that an explicit solution of the form $y = y(t;\epsilon)$ is possible only if

$$\phi_{yy}(t, y)|_{y(t;\epsilon)} \neq 0. \tag{4.2}$$

Such a condition ensures that at each time t only one characteristic curve $\phi(t, y(t, \epsilon))$ is tangent to the shoreline $x_s(t)$ (that is only one solution of (3.3) exists). Then, the

condition

$$\phi_{yy}(t, y)|_{y(t;\epsilon)} = 0 \tag{4.3}$$

represents the breaking condition at the shoreline. As a consequence, since we assume the seaward data to be small and know that waves become steeper as they travel shoreward, we can assume that non-breaking waves at the shoreline imply non-breaking waves all over the domain (see, for example, Meyer 1986*a*). Given that $\phi_{yy}^{(0)} = -1/2$, the condition for non-breaking waves at the shoreline is directly obtained from (4.2) and reads

$$\phi_{yy}(t, y)|_{y(t;\epsilon)} < 0. \tag{4.4}$$

Starting from (4.4) and using a perturbation approach, we can easily get a first-order breaking condition. From §3.1.1, we know that $\phi_y = 0$ is equivalent to $y(t) = y_0(t) + O(\epsilon)$. Hence, evaluating ϕ_{yy} at $y(t) = y_0(t) + O(\epsilon)$, we get

$$\phi_{yy}(t, y(t)) = -\frac{1}{2} + \epsilon\phi_{yy}^{(1)}(t, y_0(t)) + O(\epsilon^2) < 0. \tag{4.5}$$

Dropping all second-order contributions and using the results of Appendix B, we get

$$\ddot{x}_s^{(1)}(t) < \frac{1}{\epsilon} + 2\dot{\alpha}_{0,1}(t-2), \tag{4.6}$$

which represents a bound to the acceleration of the first-order shoreline. Then, the breaking condition becomes

$$\max_{t\in\mathbb{R}} \left[\ddot{x}_s^{(1)}(t) - 2\dot{\alpha}_{0,1}(t-2)\right] < \frac{1}{\epsilon}. \tag{4.7}$$

Considering the periodic datum in (3.23), it is possible to find an explicit expression for (4.7). As shown in Appendix B, we get

$$\sqrt{a^2(\omega) + b^2(\omega)} < \frac{1}{\epsilon} \quad \Rightarrow \quad \epsilon < \frac{1}{\sqrt{a^2(\omega) + b^2(\omega)}}, \tag{4.8}$$

where

$$a(\omega) = \left[\frac{-2\omega^2 J_0(2\omega)}{J_0^2(2\omega) + J_1^2(2\omega)} - 4\omega\sin(2\omega)\right], \quad b(\omega) = \left[\frac{-2\omega^2 J_1(2\omega)}{J_0^2(2\omega) + J_1^2(2\omega)} + 4\omega\cos(2\omega)\right].$$

Condition (4.8) gives a bound to the wave amplitude as a function of the steepness parameter ω. In figure 16 we show such a bound as a curve in the space of the parameters (ϵ, ω); below such a curve the wave is non-breaking. We also report the breaking curve as predicted by the second-order solution of Antuono & Brocchini (2007, 2008). It is evident that the match is excellent and that the first-order condition given by the present model is equivalent to the second-order condition provided by the hodographic model of Antuono & Brocchini (2007).

5. Conclusions

The BVP for the NSWEs has been first elucidated in detail and subsequently solved by means of physical variables.

The present model provides solutions for the near-shoreline flows which offer a better compromise in terms of completeness (a BVP is solved instead of the typically analysed initial value problem), accuracy (the perturbation approach makes it possible

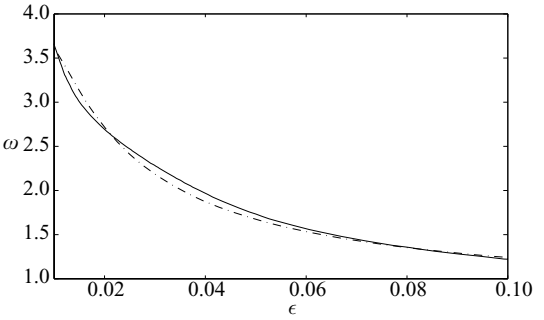

FIGURE 16. Comparison between the first-order breaking curve for the periodic datum in (3.23) (solid line) and the second-order breaking curve predicted by the model of Antuono & Brocchini (2007, 2008; dot-dashed line).

to retain the main nonlinear features of the wave propagation) and simplicity (no hodograph transformation is needed) than any other analytical model currently available for the NSWEs.

Analytical results are available at both first-order and second-order levels of expansion in terms of a small-amplitude parameter ϵ. Some sample waves, which characterize both periodic conditions (sinusoidal waves) and pulse-like conditions (solitary waves), are analysed in detail for illustrative purposes. For these waves, first-order and first-half-order solutions of the shoreline motion and of the near-shoreline flows are computed, illustrated and successfully compared with the second-order solutions obtained by the hodograph transformation method of Antuono & Brocchini (2007).

Solution of the BVP also allows for direct inspection of the flow evolution at the seaward boundary and within the domain in which interaction of the incoming and outgoing signals is accurately modelled and illustrated.

Finally, analytical conditions which describe the phenomenon of wave breaking within the domain are provided. These have been compared with those computed on the basis of the hodograph transformation method of Antuono & Brocchini (2007), showing that the first-order condition of the present model is comparable to the second-order condition of that model.

This and the fact that the sample first-half-order computations favourably compare with the second-order solutions of Antuono & Brocchini (2007) testify to how the present model provides a useful practical tool of computation even at a low order in ϵ. However, the present model enables a straightforward computation (albeit one involving a tedious programming task) of the main flow variables at the second order of accuracy in ϵ by direct substitution of the available second-order solution $\phi^{(2)}$ in the expressions of the properties of interest (e.g. x_s, u_s).

The present approach to the solution of the BVPs not only represents a significant step forward in the analytical solution of near-shoreline flow problems but also provides useful benchmarks for testing both simpler analytical solutions and numerical solvers for near-shore flows.

This work was partially funded by the Italian Ministero dei Trasporti within the framework of the 'Programma di Ricerca INSEAN 2007-2009' and Programma sulla Sicurezza INSEAN 2009'.

Appendix A. Theoretical foundations

A.1. *Regularity of solution (2.26)*

We here prove solution (2.26) to be regular as $\tau \to 0$. We consider only the inner integral of the second term in (2.26). It can be separated in two parts

$$T_1 = N_J(s\tau) \int_0^\tau sz N_K(sz)\, \mathrm{e}^{-\mathrm{i}sz} \hat{F}(z, s)\, \mathrm{d}z, \tag{A 1a}$$

$$T_2 = sN_K(s\tau) \int_0^\tau z N_J(sz)\, \mathrm{e}^{-\mathrm{i}sz} \hat{F}(z, s)\, \mathrm{d}z. \tag{A 1b}$$

We note that $N_J(x)$ is a regular function, while $N_K(x)$ has a singularity at $x = 0$ (see Abramowitz & Stegun 1964). We assume $\hat{F}(z, s)$ to be a regular function of both s and z and focus our attention on T_1. If $\tau \to 0$, then $z \to 0$, and since we have

$$\lim_{x \to 0} x N_K(x) = -\mathrm{i},$$

we have proven that T_1 is regular at both $\tau = 0$ and $s = 0$. Now we can consider T_2. If we take the limit $s \to 0$, following the previous proof we can state that T_2 has a regular limit. More complex is the proof for $\tau \to 0$. We first note that the integral contained in T_2 is a regular function of τ, and then we expand it in a Taylor series, obtaining

$$\int_0^\tau z N_J(sz)\, \mathrm{e}^{-\mathrm{i}sz} \hat{F}(z, s)\, \mathrm{d}z = \hat{F}(0, s)\tau^2 + O(\tau^3).$$

Hence, for small τ, T_2 can be rewritten in the following way:

$$T_2 = sN_K(s\tau)\hat{F}(0, s)\tau^2 + O(\tau^2),$$

Therefore, it shows a regular limit for $\tau \to 0$. We also note that both T_1 and T_2 go to zero for $\tau \to 0$.

A.1.1. *Consistency of the results*

Since we have assumed the solution domain to be $(\tau, \xi) \in (-2, \infty) \times \mathbb{R}$, we have to note that (2.23) and (2.26) are, actually, unbounded for $\tau \to +\infty$. The same behaviour is shown by the trivial solution since $\phi^{(0)} = -\tau^2/4$. This seems to invalidate the perturbation expansion; however, this is not the case. First of all, the leading term for $\tau \to +\infty$ is given by the trivial solution; we have $\phi^{(0)} \to -\infty$. This ensures that for each characteristic curve there exists a finite time for which the curve reaches the seaward boundary again and then travels out of the sloping zone. If we denote this special time by $\tilde{\tau}(\xi)$, we have that the actual domain of the solution is $(\tau, \xi) \in (-2, \tilde{\tau}(\xi)) \times \mathbb{R}$, that is a strip of the (τ, ξ)-plane. We can also give an estimate of such a time by assuming, as usual, $\tilde{\tau}(\xi) = \tilde{\tau}_0(\xi) + \epsilon\tilde{\tau}_1(\xi) + O(\epsilon^2)$. We obtain

$$\tilde{\tau}_0(\xi) = 2, \quad \tilde{\tau}_1(\xi) = \phi^{(1)}(\tilde{\tau}_0(\xi), \xi) = \phi^{(1)}(2, \xi). \tag{A 2}$$

Since in the strip domain $\phi^{(n)}$ is, actually, bounded, $\forall n \geqslant 0$, we have that the perturbation expansion is well posed.

A.1.2. *An ill-posed problem*

The BVP with the only assignment on $\phi|_{t=y}$ is an ill-posed problem. To prove this, we consider the following expression:

$$\phi(t, y) = -\frac{(t + y - 2\alpha(y))}{2}(t - y) - 1. \tag{A 3}$$

It is easy to prove that (A 3) is a solution of (2.9) which satisfies the boundary condition $\phi|_{t=y} = -1$ but does not reduce to the trivial solution $\phi^{(0)}$ when $\alpha(y) = 2 + y$ (that is when the trivial case is considered). This means that the solution of the BVP is not unique. However, the solution in (A 3) has not been considered, since being different from $\phi^{(0)}$, it has no physical meaning.

Appendix B. Breaking conditions: details of derivation

In order to compute the first-order breaking condition, we evaluate $\phi^{(1)}_{yy}$:

$$\phi^{(1)}_{yy} = \frac{1}{2\pi}\int_{\mathbb{R}} \frac{e^{ist}\mathscr{F}(\alpha_{0,1})}{J_0(2s)+iJ_1(2s)}\left\{\left[\frac{is}{(t-y-2)} - s^2\right][J_0(s(t-y-2)) - iJ_1(s(t-y-2))] - 2i\frac{J_1(s(t-y-2))}{(t-y-2)^2}\right\} ds - \dot{\alpha}_{0,1}(y) + \frac{(t-y-2)}{2}\ddot{\alpha}_{0,1}(y). \tag{B 1}$$

Using $\tau = t - y - 2$ and the fact that $J_1(s\tau) = s\tau/2 + O(\tau^3)$ and $J_0(s\tau) = 1 + O(\tau^2)$ for $\tau \to 0$ (see Abramowitz & Stegun 1964), we get the following expansion for the contribution, given in curly brackets, to the integral kernel above:

$$\left(\frac{is}{\tau} - s^2\right)[J_0(s\tau) - iJ_1(s\tau)] - 2i\frac{J_1(s\tau)}{\tau^2} = \left(-\frac{s^2}{2}\right) + O(\tau).$$

Consequently, it is

$$\lim_{y\to y_0(t)} \phi^{(1)}_{yy}(t, y) = \frac{1}{2\pi}\int_{\mathbb{R}} \frac{e^{ist}\mathscr{F}(\alpha_{0,1})}{J_0(2s) + iJ_1(2s)}\left(-\frac{s^2}{2}\right) ds - \dot{\alpha}_{0,1}(t-2)$$

$$= \frac{\ddot{x}^{(1)}_s(t)}{2} - \dot{\alpha}_{0,1}(t-2). \tag{B 2}$$

Now, let us consider the periodic datum in (3.23). It is

$$\mathscr{F}(\alpha_{0,1}) = \mathscr{F}\left(2\eta^I_0\right) = 2\pi[\delta(s-\omega) + \delta(s+\omega)], \tag{B 3}$$

where δ is the Dirac delta 'function'. Then the explicit solution for $\phi^{(1)}$ is

$$\phi^{(1)}(t, y) = \frac{2}{J_0^2(2\omega)+J_1^2(2\omega)}\{J_0(\omega(t-y-2))[\cos(\omega t)J_0(2\omega) + \sin(\omega t)J_1(2\omega)] + J_1(\omega(t-y-2))[\sin(\omega t)J_0(2\omega) - \cos(\omega t)J_1(2\omega)]\} + (t-y-2)\cos(\omega y). \tag{B 4}$$

Evaluating the previous expression at $y_0 = t - 2$, we, finally, get

$$x^{(1)}_s(t) = 2\frac{\cos(\omega t)J_0(2\omega) + \sin(\omega t)J_1(2\omega)}{J_0^2(2\omega) + J_1^2(2\omega)}. \tag{B 5}$$

Such a solution allows for an explicit expression of (4.6). We get

$$a(\omega)\cos(\omega t) + b(\omega)\sin(\omega t) < \frac{1}{\epsilon}, \tag{B 6}$$

where

$$a(\omega) = \left[\frac{-2\omega^2 J_0(2\omega)}{J_0^2(2\omega) + J_1^2(2\omega)} - 4\omega\sin(2\omega)\right], \quad b(\omega) = \left[\frac{-2\omega^2 J_1(2\omega)}{J_0^2(2\omega) + J_1^2(2\omega)} + 4\omega\cos(2\omega)\right].$$

The inequality in (B 6) can be regarded as the dot-product between the vector $(a(\omega), b(\omega))$ and the unit vector $(\cos(\omega t), \sin(\omega t))$ and, therefore, can be written in the

following way:

$$\sqrt{a^2(\omega) + b^2(\omega)}\cos(\vartheta(t,\omega)) < \frac{1}{\epsilon}, \tag{B 7}$$

where $\vartheta(t,\omega)$ represents the angle between the vectors. This inequality immediately implies the first-order condition in (4.8).

REFERENCES

Abramowitz, M. & Stegun, I. 1964 *Handbook of Mathematical Functions*. Dover.

Antuono, M. & Brocchini, M. 2007 The boundary value problem for the nonlinear shallow water equation. *Stud. Appl. Maths.* **119** 71–91.

Antuono, M. & Brocchini, M. 2008 Maximum run-up, breaking conditions and dynamical forces in the swash zone: a boundary value approach. *Coast. Engng* **55** (9), 732–740.

Bellotti, G. & Brocchini, M. 2002 On using Boussinesq-type equations near the shoreline: a note of caution. *Ocean Engng* **29** 1569–1575.

Brocchini, M. & Peregrine, D. H. 1996 Integral flow properties of the swash zone and averaging. *J. Fluid Mech.* **317** 241–273.

Carrier, G. F. & Greenspan, H. P. 1958 Water waves of finite amplitude on a sloping beach. *J. Fluid Mech.* **4**, 97–109.

Hubbard, M. E. & Dodd, N. 2002 A two-dimensional numerical model of wave run-up and overtopping. *Coast. Engng* **47**, 1–26.

Mei, C. C. 1983 *The Applied Dynamics of Ocean Surface Waves*. John Wiley.

Meyer, E. R. 1986*a* On the shore singularity of water waves. Part I. The local model. *Phys. Fluids* **29** (10), 3152–3163.

Meyer, E. R. 1986*b* On the shore singularity of water waves. Part II. Small waves do not break on gentle beaches. *Phys. Fluids* **29** (10), 3164–3171.

Pritchard, D. & Dickinson, L. 2007 The near-shore behaviour of shallow-water waves with localized initial conditions. *J. Fluid Mech.* **591**, 413–436.

Shen, M. C. & Meyer, E. R. 1963 Climb of a bore on a beach. Part 3. Run-up. *J. Fluid Mech.* **16**, 113–125.

Synolakis, C. E. 1987 The run-up of solitary waves. *J. Fluid Mech.* **185**, 523–545.

Tuck, E. O. & Hwang, L. S. 1972 Long wave generation on a sloping beach. *J. Fluid Mech.* **51**, 449–461.

Whitham, G. B. 1974 *Linear and Nonlinear Waves*. Wiley.